

Protonation and Methylation of Zerovalent Molybdenum Complexes of the Types *trans*-[Mo(CNR)(L)(Ph₂PCH₂CH₂PPh₂)₂] (R = Ph or Buⁿ; L = N₂, CO, or Nitrile) and *trans*-[Mo(CO)(L')(Ph₂PCH₂CH₂PPh₂)₂] (L' = N₂ or Nitrile) To Give Carbyne or Hydrido Complexes¹

Hidetake Seino,[†] Daigo Nonokawa,[†] Goh Nakamura,^{†,‡} Yasushi Mizobe,^{*,†,§} and
 Masanobu Hidai^{*,‡}

*Institute of Industrial Science, The University of Tokyo, Roppongi, Minato-ku, Tokyo 106-8558,
 Japan, Department of Chemistry and Biotechnology, Graduate School of Engineering,
 The University of Tokyo, Hongo, Bunkyo-ku, Tokyo 113-8656, Japan, and Institute for
 Molecular Science, Myodaiji, Okazaki 444-8585, Japan*

Received January 20, 2000

Treatment of *trans*-[Mo(CNPh)(N₂)(dppe)₂] with aqueous HBF₄ afforded an aminocarbyne complex, which was isolated as *trans*-[Mo(≡CNHPh)(O=CMe₂)(dppe)₂][BF₄] (**7**) after crystallization of the crude product from acetone–hexane, whereas the reaction of *trans*-[Mo(CNBuⁿ)(N₂)(dppe)₂] with [Me₂OH][BF₄] resulted in the formation of the aminocarbene complex with an agostic α-C–H bond, *trans*-[MoF(CHNHBUⁿ)(dppe)₂][BF₄]. Analogous treatment of *trans*-[Mo(CNR)(L)(dppe)₂] (R = Ph, Buⁿ; L = *p*-MeOC₆H₄CN, CO (**4**)) with [Me₂OH][BF₄] gave aminocarbyne complexes *trans*-[Mo(≡CNHR)(NCC₆H₄OMe-*p*)(dppe)₂][BF₄] and *cis*-[Mo(≡CNHR)(CO)(dppe)₂][BF₄] (**10**). In solution at room temperature, the latter complexes gradually isomerized to the hydrido complexes [MoH(CNR)(CO)(dppe)₂][BF₄] (**12**). Related aminocarbyne complexes *cis*-[Mo(≡CNMeR)(CO)(dppe)₂][BF₄] (**13**) were obtained from the reactions of **4** with [Me₃O][BF₄]. For comparison, carbonyl complexes *trans*-[Mo(CO)(N₂)(dppe)₂] and *trans*-[Mo(CO)(*p*-MeOC₆H₄CN)(dppe)₂] were allowed to react with aqueous HBF₄, which revealed the formation of the hydrido complexes [MoH(CO)(H₂O)(dppe)₂][BF₄] (**14**) and [MoH(CO)(*p*-MeOC₆H₄CN)(dppe)₂][BF₄] (**15**), respectively. The X-ray analyses were undertaken to determine the detailed structures for **7**, **10a** (R = Ph), **12a** (R = Ph), **13b** (R = Buⁿ), **14**·THF, and **15**·Et₂O.

Introduction

Previous studies in this and other laboratories about the reactivities of Mo and W dinitrogen complexes of the type [M(N₂)₂(P)₄] (M = Mo, W; P = tertiary phosphine) have shown that the coordinated N₂ in these complexes is susceptible to the electrophilic attack by protons to be converted into a hydrazido(2–) ligand (NNH₂) and/or nitrogen hydrides, i.e., NH₃ and less commonly N₂H₄, depending on the nature of the proton source and the ancillary ligand P along with the reaction conditions.² These findings are of great importance owing to their possible relevance to the mechanism for a biological N₂ fixation in nitrogenase that still remains to be elucidated.³ Hence, reactivities of other

nitrogenase substrates such as isocyanides and nitriles bound to the {M(P)₄} chromophore have also been attracting considerable interest. In contrast to the biological catalysis of nitrogenase, which reduces MeNC into methane, methylamine, and dimethylamine together with a small amount of ethylene and ethane^{3b} and transforms the nitriles RCN (R = Me, Et, Prⁿ) into the alkanes RCH₃ and ammonia,⁴ the reactions of the isocyanide complexes *trans*-[M(CNMe)₂(dppe)₂] (dppe = Ph₂PCH₂CH₂PPh₂) with 2 equiv of acid such as [Et₂OH][BF₄] and HCl have been shown to give the alkyne complexes *trans*-[MX(η²-MeHNC≡CNHMe)(dppe)₂]⁺ (X = F, Cl) via the aminocarbyne species *trans*-[M(≡C-NHMe)₂(dppe)₂]²⁺ generated by the protonation at the isocyanide N atoms,⁵ while the protonation of the dinitrogen–nitrile complexes *trans*-[M(N₂)(NCR)(dppe)₂]

[†] Institute of Industrial Science.

[‡] Department of Chemistry and Biotechnology.

[§] Institute for Molecular Science.

(1) Preparation and Properties of Molybdenum and Tungsten Dinitrogen Complexes. 67. Part 66: Seino, H.; Mizobe, Y.; Hidai, M. *Bull. Chem. Soc. Jpn.* **2000**, *73*, 631.

(2) (a) Hidai, M.; Mizobe, Y. *Chem. Rev.* **1995**, *95*, 1115. (b) Bazhenova, T. A.; Shilov, A. E. *Coord. Chem. Rev.* **1995**, *144*, 69. (c) Leigh, G. J. *Acc. Chem. Res.* **1992**, *25*, 178, and references therein.

(3) (a) Howard, J. B.; Rees, D. C. *Chem. Rev.* **1996**, *96*, 2965. (b) Burgess, B. K.; Lowe, D. J. *Chem. Rev.* **1996**, *96*, 2983. (c) Eady, R. R. *Chem. Rev.* **1996**, *96*, 3013, and references therein.

(4) Burgess, B. K. In *Molybdenum Enzymes*; Spiro, T. G., Ed.; John Wiley & Sons: New York, 1985; p 161.

(5) (a) Wang, Y.; Fraústo da Silva, J. J. R.; Pombeiro, A. J. L.; Pellinghelli, M. A.; Tiripicchio, A.; Henderson, R. A.; Richards, R. L. *J. Chem. Soc., Dalton Trans.* **1995**, 1183. See also to refer to the protonation on the related isocyanide complexes: Henderson, R. A.; Pombeiro, A. J. L.; Richards, R. L.; Fraústo da Silva, J. J. R.; Wang, Y. *J. Chem. Soc., Dalton Trans.* **1995**, 1193. (b) Formation of the aminocarbyne ligand has also been observed for the protonation reactions of a wider range of isocyanide complexes. See ref 16.

(R = Me, aryl) with excess amounts of aqueous HCl and HBF₄ has turned out to occur at the nitrile carbon to give the imido complexes *trans*-[MX(≡NCH₂R)(dppe)₂]⁺ (X = Cl, F).⁶ However, reactions of protic acids with these M(0) complexes tend to be significantly affected by subtle factors, which result in the formation of more diversified products. Thus, treatment of *trans*-[M(N₂)(NCPrⁿ)(dppe)₂] with H₂SO₄ in THF at 0 °C was reported to cause the protonation at the N₂ ligand, affording [M(NNH₂)(NCPrⁿ)(dppe)₂]²⁺.⁷ On the other hand, it has been observed that hydrido complexes [MH-(CNR)₂(dppe)₂]⁺ and hydridoaminocarbyne complexes [MH(≡CNHR)(CNR)(dppe)₂]²⁺ are formed from the reactions of *trans*-[M(CNR)₂(dppe)₂] with acids under certain controlled conditions.⁸ Formation of the former hydridobis(isocyanide) complexes is reminiscent of the reaction of *trans*-[W(N₂)₂(dppe)₂] with HCl in THF giving the hydridobis(dinitrogen) complex [WH(N₂)₂(dppe)₂]⁺.⁹ Interestingly, the reactions of the dinitrogen–nitrile complexes with the other electrophiles such as PhCOCl¹⁰ and Me₃SiI¹¹ occur rather at the N₂ ligand to give the diazenido (MNNCOPh, MNNSiMe₃) complexes or the hydrazido(2–) (MNNHCOPh, MNNH–SiMe₃) complexes resulting from the successive protonation of the produced diazenido species by adventitious HX (X = Cl, I).

In the preceding papers,¹² we have reported that a range of isocyanide–dinitrogen complexes *trans*-[Mo-(CNR)(N₂)(dppe)₂] (**1**; R = alkyl, aryl) can readily be prepared from the reactions of *trans*-[Mo(N₂)₂(dppe)₂] (**2**) with corresponding benzaldehyde imines PhCH=NR. Furthermore, a series of isocyanide complexes *trans*-[Mo(CNR)(L)(dppe)₂] (L = nitrile (**3**), CO(**4**), isocyanide, and H₂) are available from **1** through subsequent replacement of the N₂ ligand by L. Now we have investigated the protonation reactions of a series of Mo(0) complexes containing one or two nitrogenase substrates as the ligand. In this paper, we wish to summarize the results of this study, demonstrating which site in complexes **3** and **4** as well as the previously reported carbonyl complexes *trans*-[Mo(CO)(L')(dppe)₂] (L' = N₂ (**5**),¹³ nitrile (**6**)¹⁴) is more susceptible to protonation.

Results and Discussion

Protonation of Isocyanide–Dinitrogen Complexes **1**. Protonation of the bis(dinitrogen) complex **2**

(6) Seino, H.; Tanabe, Y.; Ishii, Y.; Hidai, M. *Inorg. Chim. Acta* **1998**, *280*, 163.

(7) Chatt, J.; Leigh, G. J.; Neukomm, H.; Pickett, C. J.; Stanley, D. R. *J. Chem. Soc., Dalton Trans.* **1980**, 121.

(8) (a) Pombeiro, A. J. L.; Richards, R. L. *Transition Met. Chem.* **1980**, *5*, 55. (b) Chatt, J.; Pombeiro, A. J. L.; Richards, R. L. *J. Chem. Soc., Dalton Trans.* **1979**, 1585.

(9) Chatt, J.; Heath, G. A.; Richards, R. L. *J. Chem. Soc., Dalton Trans.* **1974**, 2074.

(10) Tatsumi, T.; Hidai, M.; Uchida, Y. *Inorg. Chem.* **1975**, *14*, 2530.

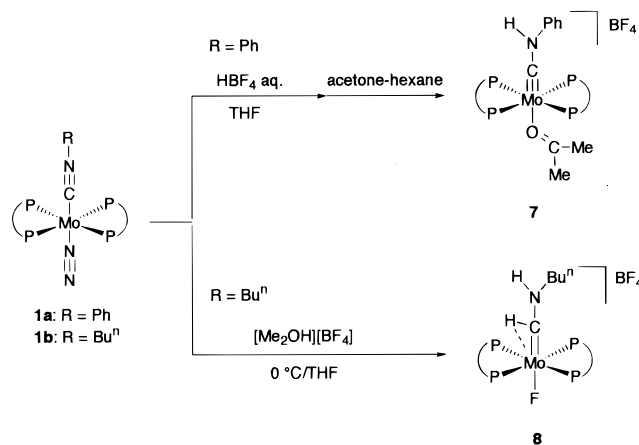
(11) Hidai, M.; Komori, K.; Kodama, T.; Jin, D.-M.; Takahashi, T.; Sugiura, S.; Uchida, Y.; Mizobe, Y. *J. Organomet. Chem.* **1984**, *272*, 155.

(12) (a) Seino, H.; Arita, C.; Nonokawa, D.; Nakamura, G.; Harada, Y.; Mizobe, Y.; Hidai, M. *Organometallics* **1999**, *18*, 4165. (b) Nakamura, G.; Harada, Y.; Arita, C.; Seino, H.; Mizobe, Y.; Hidai, M. *Organometallics* **1998**, *17*, 1010.

(13) Sato, M.; Tatsumi, T.; Kodama, T.; Hidai, M.; Uchida, T.; Uchida, Y. *J. Am. Chem. Soc.* **1978**, *100*, 4447.

(14) Tatsumi, T.; Tominaga, H.; Hidai, M.; Uchida, Y. *J. Organomet. Chem.* **1980**, *199*, 63.

Scheme 1



by aqueous HBF₄ in THF has already been reported by this group to proceed at the terminal N atom of one N₂ ligand, affording the doubly protonated product *trans*-[MoF(NNH₂)(dppe)₂][BF₄].¹⁵ Now we have found that the analogous treatment of the isocyanide–dinitrogen complex **1a** (R = Ph) results in the formation of an aminocarbyne complex; that is, monoprotection occurs not at the N₂ ligand but at the isocyanide N atom. There is precedent that the addition of electrophiles to electron-rich isocyanide complexes results in the formation of aminocarbyne complexes.¹⁶ Molecular orbital calculations on the related d⁶ electron-rich Re isocyanide complex [ReCl(CNH)(H₂PCH₂CH₂PH₂)₂] were carried out previously, which demonstrated that a negative charge is accumulated on the Cl and N atoms and the reaction with the electrophile gives the product of N attack, that is, the thermodynamically favored aminocarbyne complex.¹⁷ The product was isolated as the acetone adduct *trans*-[Mo(≡CNHPh)(Me₂CO)(dppe)₂][BF₄] (**7**) after recrystallization of the yet uncharacterizable crude product¹⁸ from acetone/hexane (Scheme 1). The IR spectrum of **7** shows a weak band at 3308 cm^{−1} attributable to ν(NH), which shifted to 2427 cm^{−1} for the deuterium analogue. In the ¹H NMR spectrum, however, the resonance due to the amino proton was not assignable presumably because of its overlapping with the phenyl resonances. The *trans* geometry around the Mo was implicated by its ³¹P NMR spectrum exhibiting only one singlet at 60.5 ppm.

Detailed structure of **7** has been determined by the X-ray crystallography. An ORTEP drawing and the important bond distances and angles are shown in Figure 1 and Table 1, respectively. Complex **7** has an octahedral configuration with the aminocarbyne and acetone ligands in mutually *trans* positions. For the aminocarbyne ligand, the Mo–C–N linkage is essentially linear (176.8(3)°). The short Mo–C distance

(15) Hidai, M.; Kodama, T.; Sato, M.; Harakawa, M.; Uchida, Y. *Inorg. Chem.* **1976**, *15*, 2694.

(16) (a) Mayr, A.; Hoffmeister, H. *Adv. Organomet. Chem.* **1991**, *32*, 227. (b) Mayr, A.; Bastos, C. M. *Prog. Inorg. Chem.* **1992**, *40*, 1. (c) Filippou, A. C. In *Organic Synthesis via Organometallics*; Helmchen, G., Dibo, J., Flubacher, D., Wiese, B., Eds.; F. Vieweg & Sohn: Braunschweig, 1997; p 97.

(17) Carvalho, M. F. N. N.; Pombeiro, A. J. L.; Bakalbassis, E. G.; Tsipis, C. A. *J. Organomet. Chem.* **1989**, *371*, C26.

(18) The crude product probably contains a H₂O molecule at the site *trans* to the aminocarbyne ligands, although full characterization was unsuccessful.

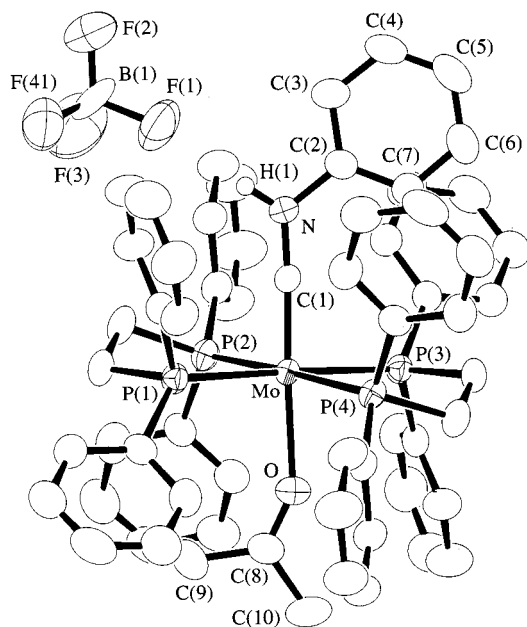


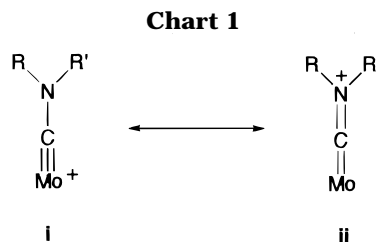
Figure 1. ORTEP drawing of **7**. Hydrogen atoms are omitted for clarity except for the amino proton H(1), having hydrogen-bonding interaction with F(1).

Table 1. Selected Bond Distances and Angles in 7

(a) Bond Distances (Å)			
Mo–P(1)	2.520(1)	Mo–P(2)	2.473(1)
Mo–P(3)	2.522(1)	Mo–P(4)	2.526(1)
Mo–O	2.310(3)	Mo–C(1)	1.808(4)
O–C(8)	1.226(5)	C(1)–N	1.345(5)
N–H(1)	0.90	F(1)–H(1)	2.12
(b) Bond Angles (deg)			
P(1)–Mo–P(2)	80.70(4)	P(1)–Mo–P(3)	178.32(5)
P(1)–Mo–P(4)	100.16(4)	P(1)–Mo–O	92.94(9)
P(1)–Mo–C(1)	89.2(1)	P(2)–Mo–P(3)	98.92(4)
P(2)–Mo–P(4)	177.63(6)	P(2)–Mo–O	94.64(8)
P(2)–Mo–C(1)	87.4(1)	P(3)–Mo–P(4)	80.16(4)
P(3)–Mo–O	85.45(9)	P(3)–Mo–C(1)	92.5(1)
P(4)–Mo–O	83.12(7)	P(4)–Mo–C(1)	94.8(1)
O–Mo–C(1)	177.3(2)	Mo–O–C(8)	152.0(3)
Mo–C(1)–N	176.8(3)	C(1)–N–C(2)	125.3(4)
C(1)–N–H(1)	126.0	C(2)–N–H(1)	108.0
F(1)–H(1)–N	149.0		

at 1.808(4) Å is diagnostic of the Mo–C multiple bonding, which is comparable to those in the other carbyne complexes,^{16a} e.g., [Mo(≡CNET₂)(CO)₃(*μ*-I)]₂ (1.80(2) Å)¹⁹ and [CpMo(≡CCH₂CMe₃)(P(OMe)₃)₂] (1.796(2) Å; Cp = η⁵-C₅H₅).²⁰ The bond angles around the N atom (125.3(4)°, 126°, and 108°) are indicative of its sp² character, which is consistent with the C(1)–N bond length at 1.345(5) Å, being much shorter than the typical C–N single bond distance of 1.47 Å. These structural features of the aminocarbene ligand may be interpreted in terms of the delocalization of electron density from the N p orbital by interaction with a p orbital on the carbyne C atom as described by the two extreme structures **i** and **ii** shown in Chart 1.²¹

The acetone ligand is bound to the Mo atom in an η^1 manner as commonly observed for the ketone complexes.



The C–O distance at 1.226(5) Å is typical of that of the C=O double bond and comparable to those in the other σ -bound acetone ligands for, for example, [Rh(=C=CPh₂)(Me₂CO)(PPRi₃)₂][PF₆] (1.216(3) Å)²² and [Ru{C(=CHPh)OCMeO}(Me₂CO)(CO)(PPRi₃)₂][BF₄] (1.235(10) Å).²³

Protonation of the Bu^nNC complex **1b** with aqueous HBF_4 under the conditions employed above did not give any characterizable products. However, protonation by the use of $[\text{Me}_2\text{OH}][\text{BF}_4]$ at 0°C proceeded cleanly, leading to the formation of the product protonated at both the N and C atoms, *trans*- $[\text{MoF}(\text{CHNHBU}^n)(\text{dppe})_2] \cdot [\text{BF}_4]$ (**8**) (Scheme 1). Differences in the reactivity between **1a** and **1b** are well comparable to those in PhNH_2 and Bu^nNH_2 arising from the stronger electron-donating ability of the Bu^n group than the Ph group. In this reaction, the second protonation seems to be so rapid that the monoprotonated product could not be detected; the ^1H NMR spectrum of the reaction mixture of **1b** with an equimolar amount of $[\text{Me}_2\text{OH}][\text{BF}_4]$ showed the presence of only **8** and unreacted **1b**. In contrast, the reaction of **1a** with $[\text{Me}_2\text{OH}][\text{BF}_4]$ was somehow elusive, and no tractable compounds were obtained from the reaction mixture.

Appearance of the four P atoms as one doublet in the $^{31}\text{P}\{^1\text{H}\}$ NMR spectrum is indicative of the trans structure for **8**, where the observed $J_{\text{P-F}}$ value of 30 Hz is in good agreement with those of related Mo complexes of the type *trans*-[MoF(E)(dppe) $_2$] $^+$ (E = NNH $_2$, 30 Hz; 15 E = NN=CHEt, 30 Hz 24). In the ^1H NMR spectrum, two new resonances each integrating for one proton appeared. One of these signals observed as a broad singlet at 3.15 ppm may be assigned to the NH proton. The other peak at -7.25 ppm, at a glance, seems to be attributable to the hydride (MoH) rather than the carbene proton (Mo=CH-), since the carbene proton is expected to resonate generally in a much lower field, e.g., 10-18 ppm. 25 However, the observed peak is correlated to the NH proton with the coupling constant of as large as 7.8 Hz, and furthermore the coupling of this resonance with the P atoms by $J_{\text{P-H}} = 10.7$ Hz seems to be too small to be assigned as that of the hydride bound to the Mo center (*vide supra*). In addition, the ^{13}C NMR spectrum showed the α -C resonance at 203.2 ppm, which split into a doublet with $J_{\text{C-H}} = 61$ Hz in the coupled spectrum. From these NMR data, it may be concluded that **1b** has a carbene ligand with an α -C-H agostic bond, as demonstrated for, for example,

(19) Fischer, E. O.; Wittman, D.; Himmelreich, D.; Cai, R.; Ackermann, K.; Neugebauer, D. *Chem. Ber.* **1982**, *115*, 3152.

(20) Allen, S. R.; Beevor, R. G.; Green, M.; Orpen, A. G.; Paddick, K. E.; Williams, I. D. *J. Chem. Soc., Dalton Trans.* **1987**, 591.

(21) (a) Kim, H. P.; Angelici, R. J. *Adv. Organomet. Chem.* **1987**, 27, 51. (b) Gallop, M. A.; Roper, W. R. *Adv. Organomet. Chem.* **1986**, 25, 121.

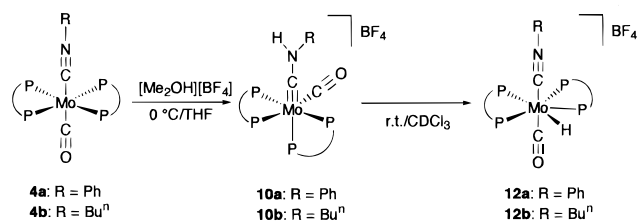
(22) Windmüller, B.; Nürnberg, O.; Wolf, J.; Werner, H. *Eur. J. Inorg. Chem.* **1999**, 613.

(23) Esteruelas, M. A.; Lahoz, F. J.; López, A. M.; Oñate, E.; Oro, L. A. *Organometallics* **1994**, *13*, 1669.

(24) Hidai, M.; Mizobe, Y.; Sato, M.; Kodama, T.; Uchida, Y. *J. Am. Chem. Soc.* **1978**, *100*, 5740.

(25) Torraca, K. E.; Ghiviriga, I.; McElwee-White, L. *Organometallics* **1999**, *18*, 2262.

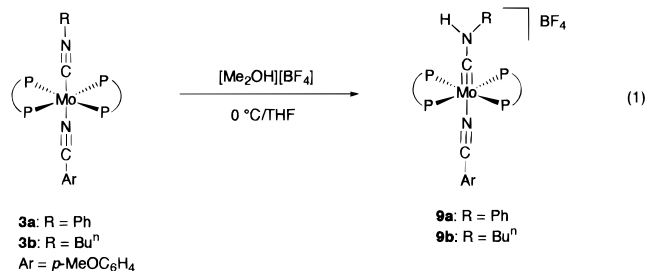
Scheme 2



[CpMo(CHBuⁿ)(CO)(P(OPh)₃)₃]⁺,²⁵ *cis*,*trans*-[W(CHR)Cl₂-(CO)(PMe₃)₂] (R = Ph,²⁶ Bu^t),²⁷ *trans*-[WCl(CHBu^t)-(PMe₃)₄]⁺,²⁸ and *trans*-[WMe(CHC₆H₄Me){PPh(CH₂CH₂-PPh₂)₂}(CO)]⁺.²⁹ The *J*_{C-H} values for such protons are reported to fall in the range 45–90 Hz, which are significantly smaller than those for the common, nonagostic methylidene protons (110–130 Hz).²⁹

Formation of an aminocarbene complex from the reaction of an isocyanide complex with excess acid is preceded. For example, [Mo(CNBU^t)₆] reacts with an excess of CF₃COOH at –78 °C to give [Mo(=CHNHBu^t)-(CNBU^t)₅][OCOCF₃]₂. However, the NMR data for this complex clearly showed the absence of any agostic interaction between the α-C–H bond and the Mo center.³⁰

Protonation of Isocyanide–Nitrile Complexes
trans-[Mo(CNR)(NCC₆H₄OMe-*p*)(dppe)₂] (**3**). The reactions of **3** with [Me₂OH][BF₄] in THF at 0 °C gave the monoprotonated products *trans*-[Mo(=CNHR)(NC-C₆H₄OMe-*p*)(dppe)₂][BF₄] (R = Ph (**9a**), Buⁿ (**9b**)) (eq 1). Only one singlet was observed in the ³¹P NMR



spectra, while two characteristic bands appeared in the IR spectra, one being assignable to $\nu(\text{C}\equiv\text{N})$ of the coordinated nitrile and the other to $\nu(\text{NH})$. These data indicate that the protonation takes place at the isocyanide N atom to give the aminocarbene ligand, which occupies the site *trans* to the nitrile ligand still intact after the reaction. The $\nu(\text{C}\equiv\text{N})$ values of 2225 and 2226 cm^{–1} observed for **9a** and **9b**, respectively, are slightly higher than that of a free *p*-MeOC₆H₄CN (2217 cm^{–1}).

Protonation of Isocyanide–Carbonyl Complexes
4. Protonation reactions of **4a** (R = Ph) and **4b** (R = Buⁿ) with [Me₂OH][BF₄] in THF at 0 °C both afforded the aminocarbene complexes *cis*-[Mo(=CNHR)(CO)-(dppe)₂][BF₄] (**10**) in moderate yields (Scheme 2). In the

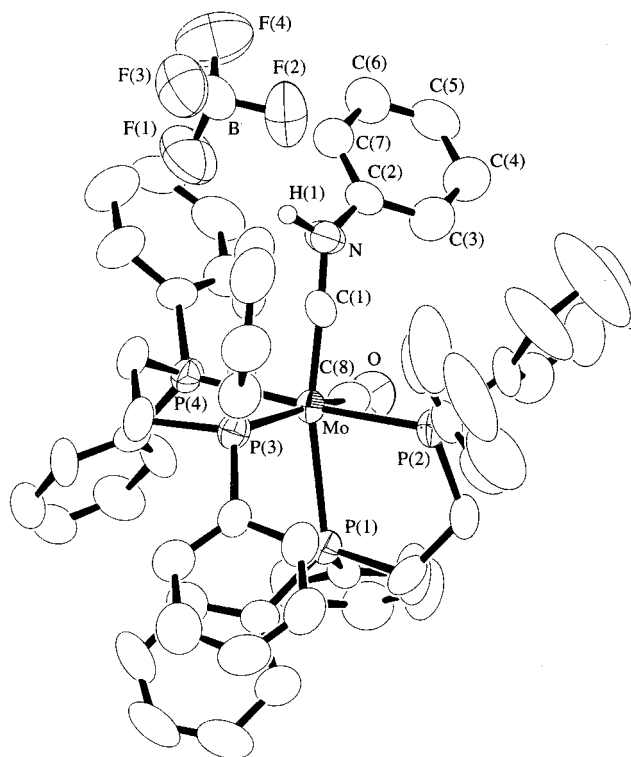


Figure 2. ORTEP drawing of **10a**. Hydrogen atoms are omitted for clarity except for the amino proton H(1), having hydrogen-bonding interaction with F(1) and F(2).

Table 2. Selected Bond Distances and Angles in **10a**

(a) Bond Distances (Å)			
Mo–P(1)	2.664(3)	Mo–P(2)	2.478(3)
Mo–P(3)	2.589(3)	Mo–P(4)	2.474(3)
Mo–C(1)	1.812(10)	Mo–C(8)	1.95(1)
C(8)–O	1.154(10)	C(1)–N	1.32(1)
N–H(1)	1.0(1)	F(1)–H(1)	2.2(1)
F(2)–H(1)	2.3(1)		
(b) Bond Angles (deg)			
P(1)–Mo–P(2)	78.66(9)	P(1)–Mo–P(3)	91.53(9)
P(1)–Mo–P(4)	105.86(9)	P(1)–Mo–C(1)	166.6(3)
P(1)–Mo–C(8)	82.2(3)	P(2)–Mo–P(3)	98.53(10)
P(2)–Mo–P(4)	174.90(10)	P(2)–Mo–C(1)	92.6(3)
P(2)–Mo–C(8)	92.1(3)	P(3)–Mo–P(4)	79.16(9)
P(3)–Mo–C(1)	99.9(3)	P(3)–Mo–C(8)	166.4(3)
P(4)–Mo–C(1)	83.4(3)	P(4)–Mo–C(8)	90.9(3)
C(1)–Mo–C(8)	88.0(4)	Mo–C(1)–N	173.3(8)
Mo–C(8)–O	178.6(10)	C(1)–N–C(2)	124.1(10)
C(1)–N–H(1)	110.0(7)	F(1)–H(1)–N	157.0(10)
F(2)–H(1)–N	134.0(9)		

IR spectra of **10**, the intense bands assignable to $\nu(\text{C}\equiv\text{O})$ appeared together with the weak $\nu(\text{NH})$ bands, indicating that the protonation occurs on the isocyanide N atom with the CO ligand intact. On the basis of the ³¹P NMR spectra exhibiting four resonances with the same intensities, the *cis* structure has been implicated for **10**.

The structure of **10a** (R = Ph) has been fully characterized by the X-ray analysis. An ORTEP drawing is depicted in Figure 2, while the important bond distances and angles are summarized in Table 2. For the aminocarbene ligand in **10a**, the Mo–C–N linkage is essentially linear (173.3(8)°), and the Mo–C and C–N distances at 1.812(10) and 1.32(1) Å are comparable to those in **7**. It is to be noted that in the closely related alkylidyne complex *cis*-[Mo(=CCH₂Ph)(CO)(dppe)₂]-

(26) Mayr, A.; Asaro, M. F.; Kjelsberg, M. A.; Lee, K. S.; Van Eugen, D. *Organometallics* **1987**, *6*, 432.

(27) Wengrovius, J. H.; Schrock, R. R.; Churchill, M. R.; Wasserman, H. J. *J. Am. Chem. Soc.* **1982**, *104*, 1739.

(28) Holmes, S. J.; Clark, D. N.; Turner, H. W.; Schrock, R. R. *J. Am. Chem. Soc.* **1982**, *104*, 6322.

(29) Jeffery, J. C.; Weller, A. S. *J. Organomet. Chem.* **1997**, *548*, 195.

(30) Carnahan, E. M.; Lippard, S. J. *J. Chem. Soc., Dalton Trans.* **1991**, 699.

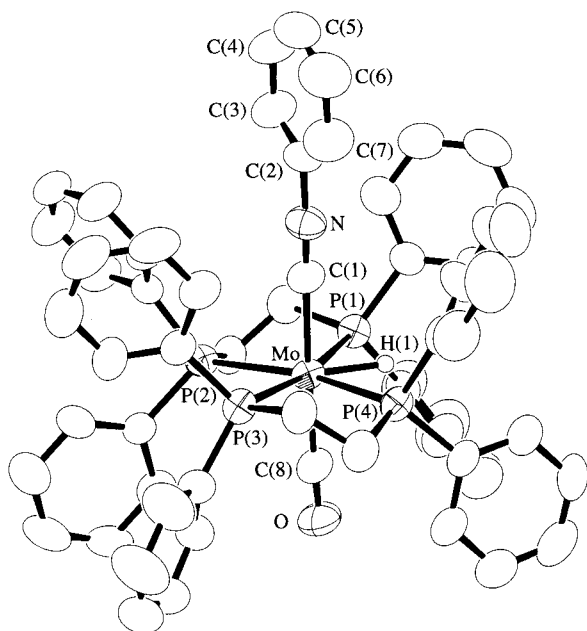


Figure 3. ORTEP drawing of the cation in **12a**. Hydrogen atoms are omitted for clarity except for the hydride H(1).

[BF₄] (**11**)³¹ the Mo–C_{carbyne} distance (1.768(8) Å) is considerably shorter than that in **10a**. This may be explained by the significant contribution of the resonance structure **ii** shown in Chart 1 for the aminocarbyne complex **10a**. The fact that the $\nu(\text{C}\equiv\text{O})$ bands appeared at 1893 and 1910 cm^{−1} for **10a** and **11**, respectively, indicates the stronger electron-donating ability of the Mo center toward the CO ligand in **10a** than that in **11**. This is also consistent with the significant contribution of structure **ii**, where the donation of lone-pair electron density occurs from the N atom toward the metal center.

Complexes **10** have proved to be unstable in solution at room temperature. Thus, **10** dissolved in CDCl₃ are gradually converted into hydridoisocyanide complexes [MoH(CNR)(CO)(dppe)₂][BF₄] (**12**) (Scheme 2). As expected, this isomerization turned out to be much enhanced by the addition of [Me₂OH][BF₄]. Migration of the proton from the aminocarbyne ligand to the metal center was invoked previously to explain the formation of [MH(CNMe)₂(dppe)₂]⁺ from the reaction of *trans*-[M(CNMe)₂(dppe)₂] and [Et₂OH][BF₄] via the presumed intermediate *trans*-[M(≡CNHMe)(CNMe)(dppe)₂]⁺.^{8a}

The structure of **12a** (R = Ph) has been determined in detail by X-ray analysis (Figure 3 and Table 3). Complex **12a** has a pentagonal bipyramidal structure with the CO and PhNC ligands occupying the apical positions. The hydride was unequivocally found in the Fourier map, which lies on the basal plane between the P(1) and P(4) atoms ($d(\text{Mo}–\text{H}) = 1.63(7)$ Å). Bonding parameters in the CO and PhNC ligands are unexceptional. The IR spectrum of **12a** shows the intense bands at 2061 and 1861 cm^{−1} assignable to $\nu(\text{C}\equiv\text{N})$ and $\nu(\text{C}\equiv\text{O})$, respectively, which are shifted to the considerably higher region than those of the parent Mo(0) complex **4a** ($\nu(\text{C}\equiv\text{N})$, 2017 and 1991; $\nu(\text{C}\equiv\text{O})$, 1812 cm^{−1}).^{12a} The ³¹P NMR spectrum of **12a** exhibits two

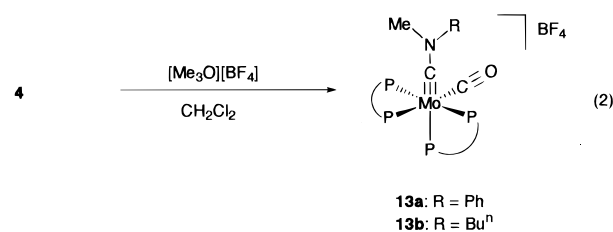
Table 3. Selected Bond Distances and Angles in **12a**

(a) Bond Distances (Å)			
Mo–P(1)	2.475(2)	Mo–P(2)	2.565(2)
Mo–P(3)	2.570(2)	Mo–P(4)	2.471(2)
Mo–C(1)	2.094(6)	Mo–C(8)	1.977(7)
C(8)–O	1.157(7)	C(1)–N	1.163(7)
Mo–H(1)	1.63(7)		
(b) Bond Angles (deg)			
P(1)–Mo–P(2)	78.70(6)	P(1)–Mo–P(3)	168.60(6)
P(1)–Mo–P(4)	112.12(6)	P(1)–Mo–C(1)	87.8(2)
P(1)–Mo–C(8)	88.9(2)	P(2)–Mo–P(3)	91.35(6)
P(2)–Mo–P(4)	168.38(6)	P(2)–Mo–C(1)	93.5(2)
P(2)–Mo–C(8)	87.5(2)	P(3)–Mo–P(4)	78.28(6)
P(3)–Mo–C(1)	87.2(2)	P(3)–Mo–C(8)	96.3(2)
P(4)–Mo–C(1)	91.2(2)	P(4)–Mo–C(8)	88.4(2)
C(1)–Mo–C(8)	176.3(3)	Mo–C(1)–N	178.4(6)
Mo–C(8)–O	178.6(6)	C(1)–N–C(2)	177.5(7)
P(1)–Mo–H(1)	50.0(2)	P(4)–Mo–H(1)	61.0(2)

broad resonances with the same intensities, while the ¹H NMR spectrum shows a high-field resonance characteristic of the hydride proton, which splits into a triplet of triplets at low temperatures. These spectral data are consistent with the solid structure clarified by the X-ray diffraction. Complex **12b** also exhibited the analogous spectral feature.

Methylation of Isocyanide–Carbonyl Complexes

4. Complexes **4** reacted with [Me₃O][BF₄] in CH₂Cl₂ at room temperature to give the aminocarbyne complexes *cis*-[Mo(≡CNMeR)(CO)(dppe)₂][BF₄] (**13**) in moderate yields (eq 2). Isolation of any characterizable products



failed by the analogous treatment of **1** with [Me₃O][BF₄]. It is interesting to note that [Mo(CNBut)₆] is susceptible to electrophilic attack by MeOTf²⁹ and alkyl halides³² at the α -carbon atom to give η^2 -iminoacyl complexes [Mo(η^2 -BuⁿCNR)(CNBu^t)₅]⁺ (R = Me, PhCH₂). Spectroscopic data for **13** are indicative of the *cis* structure, as manifested for the related CNHR complexes **10**, which has been confirmed by X-ray analysis of the Buⁿ complex **13b**.

An ORTEP drawing of the cation in **13b** is shown in Figure 4, while selected bond distances and angles are listed in Table 4. The structure of **13b** is quite analogous to that of **10a**. Thus, the aminocarbyne and CO ligands occupy the mutually *cis* positions, and in the aminocarbyne ligand the Mo–C–N linkage is almost linear (173.7(6)°). However, the Mo–C distance at 1.843(7) Å is slightly longer and the C_{carbyne}–N distance at 1.305(8) Å is a little shorter than the corresponding bond distances of 1.812(10) and 1.32(1) Å, respectively, in **10a**. These differences may be explained by the greater contribution of the structure **ii** for **13b** with the strongly electron-donating NBuⁿMe group than for **10a** with the NPh moiety. The almost planar geometry around the

(31) Nakamura, G.; Harada, Y.; Mizobe, Y.; Hidai, M. *Bull. Chem. Soc. Jpn.* **1996**, *69*, 3305.

(32) Yoshida, T.; Hirotsu, K.; Higuchi, T.; Otsuka, S. *Chem. Lett.* **1982**, 1017.

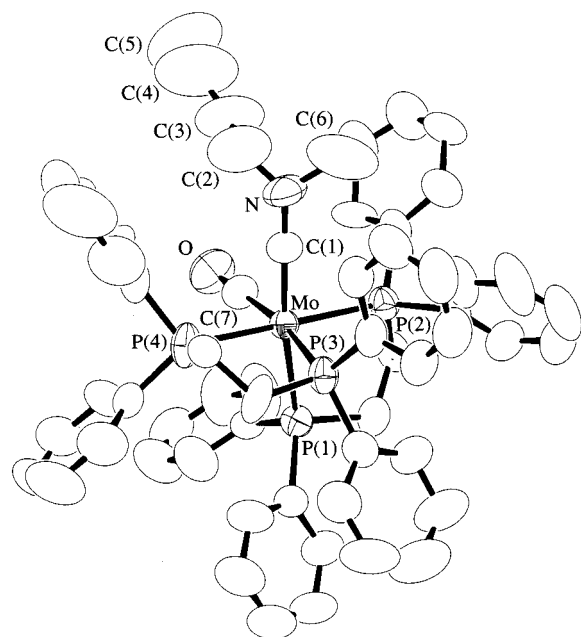


Figure 4. ORTEP drawing of the cation in **13b**. Hydrogen atoms are omitted for clarity.

Table 4. Selected Bond Distances and Angles in 13b

(a) Bond Distances (Å)			
Mo–P(1)	2.664(2)	Mo–P(2)	2.501(2)
Mo–P(3)	2.589(2)	Mo–P(4)	2.502(2)
Mo–C(1)	1.843(7)	Mo–C(7)	1.950(7)
C(7)–O	1.169(7)	C(1)–N	1.305(8)

(b) Bond Angles (deg)			
P(1)–Mo–P(2)	78.82(6)	P(1)–Mo–P(3)	95.36(6)
P(1)–Mo–P(4)	102.32(7)	P(1)–Mo–C(1)	165.3(2)
P(1)–Mo–C(7)	83.9(2)	P(2)–Mo–P(3)	99.15(6)
P(2)–Mo–P(4)	177.92(7)	P(2)–Mo–C(1)	89.4(2)
P(2)–Mo–C(7)	91.2(2)	P(3)–Mo–P(4)	79.05(6)
P(3)–Mo–C(1)	95.2(2)	P(3)–Mo–C(7)	169.3(2)
P(4)–Mo–C(1)	89.7(2)	P(4)–Mo–C(7)	90.7(2)
C(1)–Mo–C(7)	87.6(3)	Mo–C(1)–N	173.7(6)
Mo–C(7)–O	177.5(6)	C(1)–N–C(2)	129.5(8)
C(1)–N–C(6)	121.0(8)	C(2)–N–C(6)	106.3(9)

N atom is observed also in **13b**, with C–N–C angles of 129.5(8)°, 121.0(8)°, and 106.3(9)°.

Protonation of Carbonyl–Dinitrogen Complex 5 and Carbonyl–Nitrile Complex 6. Relevant to the reaction of isocyanide–carbonyl complexes **4** with [Me₂OH][BF₄], our study has been extended further to clarify the details of the protonation reactions of other Mo(0) carbonyl complexes. As for the related reaction of *cis*-[Mo(CO)₂(dppe)₂] with acids, the hydrido complex [MoH(CO)₂(dppe)₂][SO₃F], having a monocapped octahedral structure, was formed by treatment with HSO₃F,³³ whereas the paramagnetic complexes *trans*-[Mo(CO)₂(dppe)₂][X] (X = BF₄, HSO₄) were obtained from the reaction with [Et₂OH][BF₄] and H₂SO₄.³⁴

Now we have found that treatment of **5** with aqueous HBF₄ in THF at room temperature results in the loss of the coordinated N₂ to give the hydrido complex [MoH(CO)(OH₂)(dppe)₂][BF₄] (**14**) (eq 3), whose structure has been determined unambiguously by X-ray analysis

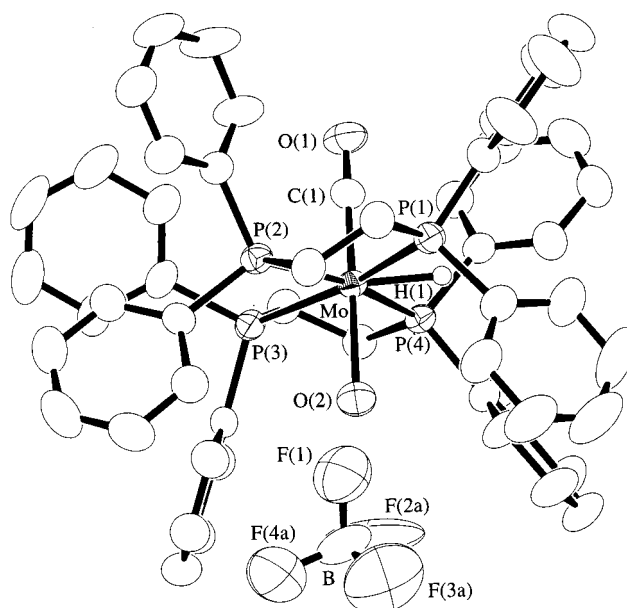


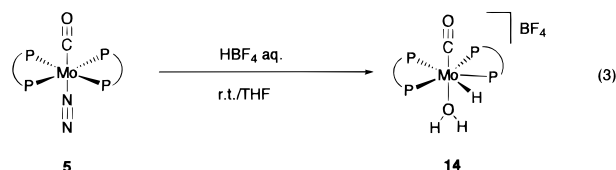
Figure 5. ORTEP drawing of **14**. Hydrogen atoms are omitted for clarity except for the hydride H(1).

Table 5. Selected Bond Distances and Angles in 14

(a) Bond Distances (Å)			
Mo–P(1)	2.453(1)	Mo–P(2)	2.575(2)
Mo–P(3)	2.516(1)	Mo–P(4)	2.426(1)
Mo–O(2)	2.330(6)	Mo–C(1)	1.857(5)
C(1)–O(1)	1.175(5)	Mo–H(1)	1.63(5)

(b) Bond Angles (deg)			
P(1)–Mo–P(2)	77.47(5)	P(1)–Mo–P(3)	167.61(5)
P(1)–Mo–P(4)	114.33(5)	P(1)–Mo–O(2)	88.68(9)
P(1)–Mo–C(1)	93.1(2)	P(2)–Mo–P(3)	90.17(4)
P(2)–Mo–P(4)	168.10(5)	P(2)–Mo–O(2)	83.0(1)
P(2)–Mo–C(1)	97.5(2)	P(3)–Mo–P(4)	78.05(4)
P(3)–Mo–O(2)	90.63(9)	P(3)–Mo–C(1)	87.7(2)
P(4)–Mo–O(2)	95.3(1)	P(4)–Mo–C(1)	83.9(2)
O(2)–Mo–C(1)	178.2(2)	Mo–C(1)–O(1)	176.5(4)
P(1)–Mo–H(1)	53.0(1)	P(4)–Mo–H(1)	60.0(1)

(Figure 5 and Table 5). No intermediate stages, e.g., a hydroxycarbene complex, were detected. Complex **14**



has a pentagonal bipyramidal geometry with the CO and H₂O ligands in the apical positions. The hydride was located between the P(1) and P(4) atoms, with the Mo–H distance at 1.63(5) Å. Complex **14** shows a strong ν(C≡O) band at 1776 cm^{−1} in its IR spectrum, which is lower than the values for [Mo(CO)(dppe)₂] (1807 cm^{−1}) and **5** (1812 and 1789 cm^{−1}).¹³ The exceptionally low ν(C≡O) value observed for the CO ligand in **14** suggests the extremely electron-donating nature of the [MoH(CO)(OH₂)(dppe)₂]⁺ moiety toward the CO ligand, having no other π-acidic ligands but the good donor ligand H₂O in the trans position.

Treatment of the carbonyl–nitrile complex *trans*-[Mo(CO)(NCC₆H₄OMe-*p*)(dppe)₂] (**6**) with aqueous HBF₄ also afforded the hydrido complex [MoH(CO)(NCC₆H₄OMe-*p*)(dppe)₂][BF₄] (**15**) in high yield (eq 4). In contrast

(33) Datta, S.; Dezube, B.; Kouba, J. K.; Wreford, S. S. *J. Am. Chem. Soc.* **1978**, *100*, 4404.

(34) Chatt, J.; Pombeiro, A. J. L.; Richards, R. L. *J. Chem. Soc., Dalton Trans.* **1980**, 492.

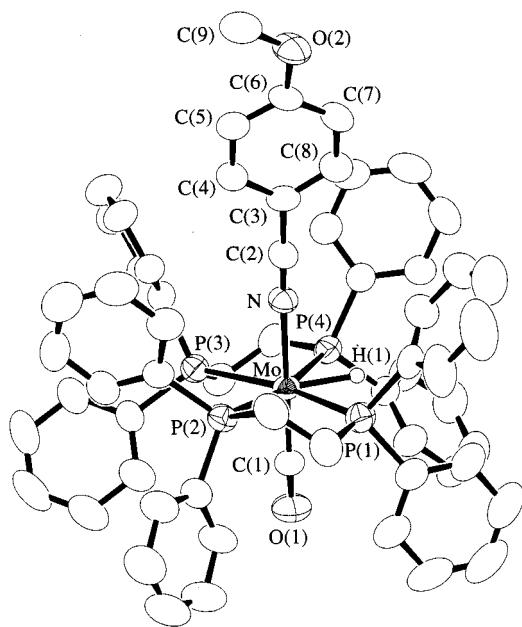
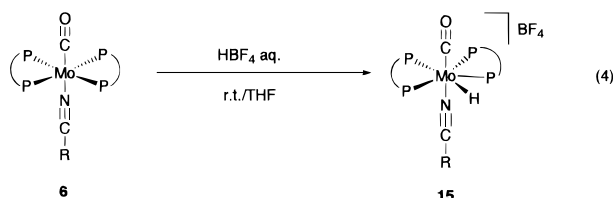


Figure 6. ORTEP drawing of the cation in **15**. Hydrogen atoms are omitted for clarity except for the hydride H(1).

Table 6. Selected Bond Distances and Angles in **15**

(a) Bond Distances (Å)			
Mo–P(1)	2.464(2)	Mo–P(2)	2.567(2)
Mo–P(3)	2.550(2)	Mo–P(4)	2.438(2)
Mo–N	2.190(4)	Mo–C(1)	1.892(5)
C(1)–O(1)	1.181(6)	N–C(2)	1.131(6)
Mo–H(1)	1.64(3)		
(b) Bond Angles (deg)			
P(1)–Mo–P(2)	77.61(5)	P(1)–Mo–P(3)	167.94(5)
P(1)–Mo–P(4)	114.49(5)	P(1)–Mo–N	90.4(1)
P(1)–Mo–C(1)	91.2(2)	P(2)–Mo–P(3)	90.73(5)
P(2)–Mo–P(4)	167.49(5)	P(2)–Mo–N	85.2(1)
P(2)–Mo–C(1)	96.8(2)	P(3)–Mo–P(4)	77.34(5)
P(3)–Mo–N	91.7(1)	P(3)–Mo–C(1)	87.0(2)
P(4)–Mo–N	91.3(1)	P(4)–Mo–C(1)	86.5(2)
N–Mo–C(1)	177.6(2)	Mo–N–C(2)	177.7(5)
Mo–C(1)–O(1)	175.8(5)	N–C(2)–C(3)	176.0(6)
P(1)–Mo–H(1)	59.0(1)	P(4)–Mo–H(1)	55.0(1)

to the reaction of the dinitrogen–nitrile complex *trans*-[Mo(N₂)(NCR)(dppe)₂] with HBF₄, giving *trans*-[MoF(NCH₂R)(dppe)₂]⁺ (vide supra), the protonation of **6** occurs at the metal center without loss of both the CO and nitrile ligands. The structure of **15** has also been



characterized by X-ray crystallography, which is depicted in Figure 6 and Table 6. The geometry around the Mo in **15** is also a pentagonal bipyramid, with the CO and nitrile ligands occupying the apical positions. The hydride was found on the basal plane between the P(1) and P(4) atoms, which is consistent with the low-temperature ¹H and ³¹P NMR spectra showing a triplet of triplets at –4.45 ppm due to the hydride proton and two broad signals with the same intensities assigned to the dppe ligands, respectively. The IR spectrum

exhibiting two characteristic bands at 2217 and 1796 cm^{–1} due to ν(N≡C) and ν(C≡O) are in agreement with the structure determined by the X-ray analysis. It is to be noted that **6** shows ν(N≡C) and ν(C≡O) bands at 2155 and 1767 cm^{–1}.¹⁴

Concluding Remarks

The present study on the protonation reaction of the Mo(0) complexes containing one or two nitrogenase substrates as the ligand has disclosed that on treatment with either [Me₂OH][BF₄] or aqueous HBF₄, a series of isocyanide complexes *trans*-[Mo(CNR)(L)(dppe)₂] with L = N₂, *p*-MeOC₆H₄CN, and CO undergoes protonation at the isocyanide N atom to give the aminocarbene complexes except for **1b** (R = Buⁿ, L = N₂), the latter of which is susceptible to attack at both the α-C and N atom in the *n*-butylisocyanide ligand, affording the carbene complex with an agostic α-C–H bond, **8**. In the aminocarbene and carbene complexes obtained here, both the nitrile and CO ligands are still intact for **9** and **10**, whereas the coordinated N₂ in **1** is lost in the products **7** and **8**. However, the aminocarbene complexes **10** with the CO ligand are unstable in a solution state at room temperature and are converted into the hydridoisocyanide complexes **12**. The methylation of the isocyanide–carbonyl complexes **4** with [Me₃O][BF₄] proceeds similarly to give the stable aminocarbene complexes **13**. By contrast, the carbonyl complexes *trans*-[Mo(CO)(L)(dppe)₂] (L = N₂, *p*-MeOC₆H₄CN) reacted with aqueous HBF₄ to afford the hydrido complexes **14** and **15**, with a loss of the N₂ ligand for the former and a retention of the nitrile ligand for the latter, respectively.

Experimental Section

General Considerations. All manipulations were done under an atmosphere of N₂ except for those stated otherwise. IR and NMR spectra were recorded on a JASCO FT/IR-420 spectrometer at room temperature and on JEOL EX-270 or LA-400 spectrometers at 20 °C, respectively. The signals due to the aromatic protons are omitted from the ¹H NMR data shown below. Elemental analyses were carried out with a Perkin-Elmer 2400 series II CHN analyzer. Amounts of solvating molecules in the products were determined by X-ray crystallography, NMR measurements, and/or GLC analysis. Complexes **1**, **3**, **4**,¹² **5**,¹³ and **6**¹⁴ were prepared according to the literature methods, whereas aqueous HBF₄, [Me₂OH][BF₄], and [Me₃O][BF₄] were commercially obtained and used as received.

Preparation of 7. To a suspension of **1a**·2C₆H₆ (223 mg, 0.217 mmol) in THF (2 mL) was added an aqueous HBF₄ solution (42%, 0.3 mL). A yellow solid immediately precipitated, which was filtered off and redissolved in acetone. Addition of hexane to the solution afforded orange crystals of **7** (162 mg, 65% yield). Anal. Calcd for C₆₂H₆₀NOBF₄P₄Mo: C, 65.22; H, 5.30; N, 1.23. Found: C, 65.26; H, 5.44; N, 1.15. IR (KBr): ν(NH), 3308; ν(C=O), 1673; ν(CN), 1495 cm^{–1}. ¹H NMR (acetone-*d*₆): δ 2.8–3.0 (m, 8H, PCH₂), 2.04 (s, 6H, Me₂C=O). ³¹P{¹H} NMR (acetone-*d*₆): δ 60.5 (s).

Preparation of 8. A suspension of **1b** (77 mg, 0.075 mmol) in THF (3 mL) was treated with [Me₂OH][BF₄] (18 μL, 0.15 mmol) at 0 °C. After stirring for 2 h, ether was added to the reaction mixture. A yellow solid deposited, which was filtered off and crystallized from CH₂Cl₂–ether at 0 °C to give orange crystals of **8** (41 mg, 49% yield). Anal. Calcd for C₅₇H₅₉NBF₅P₄Mo: C, 63.17; H, 5.49; N, 1.29. Found: C, 63.09; H, 5.38; N,

1.54. IR (KBr): $\nu(\text{NH})$, 3360 and 3300; $\nu(\text{CN})$, 1526 cm^{-1} . ^1H NMR (CD_2Cl_2): δ -7.25 (d quin, $J_{\text{H-H}} = 7.8$ Hz, $J_{\text{H-P}} = 10.7$ Hz, 1H, MoCH), 0.50 (m, 2H, NCH_2CH_2), 0.55–0.7 (m, 5H, CH_2CH_3), 1.91 (br quar, 2H, $J = 6.8$ Hz, NCH_2), 3.15 (br, 1H, NH), 2.5–2.8 (m, 8H, PCH_2). $^{31}\text{P}\{^1\text{H}\}$ NMR (CD_2Cl_2): δ 48.6 (d, $J_{\text{P-F}} = 30$ Hz). ^{13}C NMR (CD_2Cl_2): δ 203.2 ($J_{\text{C-P}} = 13$ Hz (quin), $J_{\text{C-F}} = 67$ Hz (d), $J_{\text{C-H}} = 61$ Hz (d), MoC).

Preparation of 9a·1/2CH₂Cl₂. Into a solution of **3a**·1/2C₆H₆ (80 mg, 0.068 mmol) in THF (3 mL) was added $[\text{Me}_2\text{OH}][\text{BF}_4]$ (18 μL , 0.148 mmol) at -30 °C under Ar. After stirring for 2 h at 0 °C, ether was added to precipitate a solid, which was filtered off and recrystallized from CH_2Cl_2 -ether to give **9a**·1/2CH₂Cl₂ as orange crystals (62 mg, 73% yield). Anal. Calcd for C_{67.5}H₆₂N₂OBClF₄P₄Mo: C, 64.38; H, 4.96; N, 2.22. Found: C, 64.28; H, 5.10; N, 2.24. IR (KBr): $\nu(\text{C}\equiv\text{N})$, 2225; $\nu(\text{NH})$, 3282 cm^{-1} . ^1H NMR (CDCl_3): δ 3.90 (s, 3H, MeO), 5.05 (br, 1H, NH), 2.3–2.7 (m, 8H, PCH_2). $^{31}\text{P}\{^1\text{H}\}$ NMR (CDCl_3): δ 65.0 (s).

Preparation of 9b. This complex was obtained in 61% yield as orange crystals from **3b** by a method similar to that for preparing **9a**. Anal. Calcd for C₆₅H₆₅N₂OBF₄P₄Mo: C, 65.23; H, 5.47; N, 2.34. Found: C, 64.60; H, 5.43; N, 2.30. IR (KBr): $\nu(\text{C}\equiv\text{N})$, 2226; $\nu(\text{NH})$, 3294 cm^{-1} . ^1H NMR (CD_2Cl_2): δ 0.7 (m, 3H, CH₃), 0.8–0.9 (m, 4H, $\text{CH}_2\text{CH}_2\text{CH}_3$), 2.3–2.7 (m, 10H, NHCH_2 and PCH_2), 3.83 (s, 3H, MeO), 3.65 (br, 1H, NH). $^{31}\text{P}\{^1\text{H}\}$ NMR (CD_2Cl_2): δ 66.8 (s).

Preparation of 10a. To a suspension of **4a** (86 mg, 0.084 mmol) in THF (3 mL) was added $[\text{Me}_2\text{OH}][\text{BF}_4]$ (21 μL , 0.17 mmol) at 0 °C. After stirring for 2 h at this temperature, ether was added to deposit the orange solid, which was filtered off and recrystallized from CH_2Cl_2 -ether at -20 °C, affording orange crystals of **10a** (38 mg, 42%). Anal. Calcd for C₆₀H₅₄N₂OBF₄P₄Mo: C, 64.82; H, 4.90; N, 1.26. Found: C, 64.22; H, 4.88; N, 1.42. IR (KBr): $\nu(\text{NH})$, 3239; $\nu(\text{C}\equiv\text{O})$, 1893; $\nu(\text{CN})$, 1502 cm^{-1} . ^1H NMR (CDCl_3): δ 1.9–3.4 (m, 8H, PCH_2), 6.60 (br s, 1H, NH). $^{31}\text{P}\{^1\text{H}\}$ NMR (CDCl_3): δ 23.8 (ddd, $J = 23$, 15, and 3 Hz, 1P), 40.8 (dd, $J = 24$ and 14 Hz, 1P), 50.5 (dd, $J = 84$ and 24 Hz, 1P), 57.7 (ddd, $J = 84$, 23, and 3 Hz, 1P).

Preparation of 10b·1/2CH₂Cl₂. This complex was obtained as yellow crystals in 62% yield from **4b** by a method similar to that for **10a**. Anal. Calcd for C_{58.5}H₅₉NOBClF₄P₄Mo: C, 61.95; H, 5.24; N, 1.23. Found: C, 62.35; H, 5.21; N, 1.16. IR (KBr): $\nu(\text{NH})$, 3253; $\nu(\text{C}\equiv\text{O})$, 1854; $\nu(\text{CN})$, 1533 cm^{-1} . ^1H NMR (CDCl_3): δ 0.64 (t, 3H, $J = 7.1$ Hz, CH₃), 0.78 (sex, $J = 7.1$ Hz, 2H, CH_2CH_3), 0.85–1.05 (m, 2H, NCH_2CH_2), 1.8–3.2 (m, 10H, NCH_2 and PCH_2), 6.35 (br s, 1H, NH). $^{31}\text{P}\{^1\text{H}\}$ NMR (CDCl_3): δ 26.6 (ddd, $J = 24$, 12, and 3 Hz), 39.6 (ddd, $J = 24$, 12, and 3 Hz), 55.4 (ddd, $J = 87$, 24, and 3 Hz), 59.7 (ddd, $J = 87$, 24, and 3 Hz).

Preparation of 12a. A CH_2Cl_2 solution of **10a** (27 mg, 9.925 mmol) was left for 31 h at 20 °C. Addition of ether to the resulting solution gave pale yellow crystals of **12a** (15 mg, 56% yield). Anal. Calcd for C₆₀H₅₄N₂OBF₄P₄Mo: C, 64.82; H, 4.90; N, 1.26. Found: C, 64.69; H, 5.31; N, 1.33. IR (KBr): $\nu(\text{N}\equiv\text{C})$, 2061; $\nu(\text{C}\equiv\text{O})$, 1861 cm^{-1} . ^1H NMR (CDCl_3 , 20 °C): δ -5.35 (m, 1H, MoH), 2.4–2.8 (m, 8H, PCH_2). ^1H NMR ($\text{THF}-d_8$, -43 °C): δ -5.46 (tt, $J_{\text{P-H}} = 70.2$ and 12.7 Hz, 1H, MoH). ^1H NMR ($\text{THF}-d_8$, 47 °C): δ -5.23 (quin, $J_{\text{P-H}} = 42.1$ Hz, 1H, MoH). $^{31}\text{P}\{^1\text{H}\}$ NMR (CDCl_3): δ 54–58 and 79–83 (br, 2P each).

Formation of 12b. Isomerization of **10b** into **12b** in a CDCl_3 solution was monitored by NMR spectra, which revealed the formation of **12b** in 95% after 8.5 h. IR (KBr): $\nu(\text{NC})$, 2113; $\nu(\text{CO})$, 1833 cm^{-1} . ^1H NMR (CD_2Cl_2): δ -5.54 (pseudo quin, $J_{\text{H-P}} = 42$ Hz, 1H, MoH), 0.65 (t, $J = 7.1$ Hz, 3H, CH₃), 0.7–0.9 (m, 4H, $\text{CH}_2\text{CH}_2\text{CH}_3$), 2.4–2.8 (m, 10H, NCH_2 and PCH_2). $^{31}\text{P}\{^1\text{H}\}$ NMR (CDCl_3): δ 52–60 and 77–84 (br, 2P each).

Preparation of 13a. Complex **4a** (61 mg, 0.059 mmol) dissolved in CH_2Cl_2 (3 mL) was treated with $[\text{Me}_3\text{O}][\text{BF}_4]$ (17 mg, 0.12 mmol) at room temperature. After stirring for 20 h, ether was added to the resulting solution, affording **13a** as pale red microcrystals (29 mg, 43% yield). Anal. Calcd for

C₆₁H₅₆N₂OBF₄P₄Mo: C, 65.08; H, 5.01; N, 1.24. Found: C, 64.63; H, 5.07; N, 1.23. IR (KBr): $\nu(\text{C}\equiv\text{O})$, 1859; $\nu(\text{CN})$, 1506 cm^{-1} . ^1H NMR (CDCl_3): δ 1.6–1.8 (m, 3H, PCH_2), 1.86 (s, 3H, NMe), 2.1–2.4 (m, 3H, PCH_2), 2.85 and 3.55 (m, 1H each, PCH_2). $^{31}\text{P}\{^1\text{H}\}$ NMR (CDCl_3): δ 22.1 (br t, $J = 22$ Hz, 1P), 34.2 (br td, $J = 21$ and 5 Hz, 1P), 50.5 (ddd, $J = 84$, 23, and 5 Hz, 1P), and 56.8 (dd, $J = 84$ and 20 Hz, 1P).

Preparation of 13b. This complex was prepared by a method essentially similar to that of **13a**: pale brown crystals, yield 55%. Anal. Calcd for C₅₉H₆₀N₂OBF₄P₄Mo: C, 64.09; H, 5.47; N, 1.27. Found: C, 63.92; H, 5.48; N, 1.28. IR (KBr): $\nu(\text{C}\equiv\text{O})$, 1858; $\nu(\text{CN})$, 1550 cm^{-1} . ^1H NMR (CDCl_3): δ 0.7–1.2 (m, 7H, $\text{CH}_2\text{CH}_2\text{CH}_3$), 2.0–3.2 (m, 10H, NCH_2 and PCH_2), 2.06 (s, 3H, NMe). $^{31}\text{P}\{^1\text{H}\}$ NMR (CDCl_3): δ 25.1 (ddd, $J = 3$, 15 and 24 Hz, 1P), 37.9 (dd, $J = 23$ and 15, 1P), 50.3 (dd, $J = 85$ and 24 Hz, 1P), and 58.8 (ddd, $J = 3$, 85 and 23 Hz, 1P).

Preparation of 14·THF. To a THF solution of **5**·1/2C₆H₆ (102 mg, 0.102 mmol) was added aqueous HBF₄ (42%, 61 mg, 0.29 mmol) at room temperature. After stirring for 0.5 h, the resultant pale yellow solution was concentrated to ca. 2.5 mL. Addition of ether gave yellow crystals of **14**·THF (88 mg, 78% yield). Anal. Calcd for C₅₇H₅₀O₃BF₄P₄Mo: C, 62.31; H, 5.41. Found: C, 62.37; H, 5.44. IR (KBr): $\nu(\text{C}\equiv\text{O})$, 1776 cm^{-1} . ^1H NMR ($\text{THF}-d_8$, 20 °C): δ -3.7 to -2.5 (v br, 1H, MoH), 2.6–3.0 (m, 8H, PCH_2). ^1H NMR ($\text{THF}-d_8$, -73 °C): δ -3.39 (quin, $J_{\text{P-H}} = 41$ Hz, 1H, MoH). $^{31}\text{P}\{^1\text{H}\}$ NMR ($\text{THF}-d_8$): δ 65–69 (br).

Preparation of 15·Et₂O. To a suspension of **6** (95 mg, 0.090 mmol) in THF (3 mL) was added aqueous HBF₄ (42%, 39 mg, 0.19 mmol) under Ar, and the mixture was stirred for 2 h. By addition of ether to the resultant solution, yellow crystals of **15**·Et₂O precipitated (100 mg, 91% yield). Anal. Calcd for C₆₅H₆₆N₂O₃BF₄P₄Mo: C, 64.21; H, 5.47; N, 1.15. Found: C, 64.31; H, 5.58; N, 1.08. IR (KBr): $\nu(\text{C}\equiv\text{N})$, 2217; $\nu(\text{C}\equiv\text{O})$, 1796 cm^{-1} . ^1H NMR ($\text{THF}-d_8$, 20 °C): δ -4.20 (quin, $J_{\text{P-H}} = 42$ Hz, 1H, MoH), 2.45–2.7 and 2.8–3.05 (m, 4H each, PCH_2), 3.83 (s, 3H, MeO). ^1H NMR ($\text{THF}-d_8$, -90 °C): δ -4.45 (tt, $J_{\text{P-H}} = 70.3$ and 11.2 Hz, 1H, MoH). $^{31}\text{P}\{^1\text{H}\}$ NMR ($\text{THF}-d_8$): δ 66–70 (br). $^{31}\text{P}\{^1\text{H}\}$ NMR ($\text{THF}-d_8$, -90 °C): δ 53–56 and 83–86 (br).

X-ray Crystallographic Studies. Single crystals of **7**, **10a**, **12a**, **13b**, **14**·THF, and **15**·Et₂O were sealed in glass capillaries under Ar and transferred to a Rigaku AFC7R diffractometer equipped with a graphite-monochromatized Mo K α source. Diffraction studies were done at room temperature. Orientation matrixes and unit cell parameters were determined by least-squares treatment of 25 reflections with $35^\circ < 2\theta < 40^\circ$. The intensities of three check reflections were monitored every 150 reflections during data collection, which revealed no significant decay for **10a**, **12a**, **13b**, **14**·THF, and **15**·Et₂O, but an almost linear decay for **7**, with an average 6.3% loss in intensities at the end of the data collection. Intensity data were corrected for Lorentz and polarization effects and for absorption (ψ scans), and for **7** decay correction was also applied. Details of crystal and data collection parameters are listed in Table 7.

Structure solution and refinements were carried out by using the teXsan program package.³⁵ The positions of the non-hydrogen atoms were determined by Patterson methods and subsequent Fourier syntheses (DIRDIF PATTY),³⁶ which were refined anisotropically by full-matrix least-squares techniques. The hydrogen atoms attached to the amino N in **7** and **10a** as well as those bound to the Mo atom in **12a**, **14**, and **15** were found from the Fourier maps, which were refined isotropically, except for the amino hydrogen in **7**. Other hydrogens were

(35) teXsan: Crystal Structure Analysis Package; Molecular Structure Corp.: The Woodlands, TX, 1985 and 1992.

(36) PATTY: Beurskens, P. T.; Admirals, G.; Beurskens, G.; Bosman, W. P.; Garcia-Granda, S.; Gould, R. O.; Smits, J. M. M.; Smykalla, C. *The DIRDIF program system*; Technical Report of the Crystallography Laboratory; University of Nijmegen: The Netherlands, 1992.

Table 7. Crystallographic Data for 7, 10a, 12a, 13a, 14·THF, and 15·Et₂O

	7	10a	12a	13a	14·THF	15·Et ₂ O
formula	C ₆₂ H ₆₀ NOBF ₄ P ₄ Mo	C ₆₀ H ₅₄ NOBF ₄ P ₄ Mo	C ₆₀ H ₅₄ NOBF ₄ P ₄ Mo	C ₅₉ H ₆₀ NOBF ₄ P ₄ Mo	C ₅₇ H ₅₉ O ₃ BF ₄ P ₄ Mo	C ₆₅ H ₆₆ NO ₃ BF ₄ P ₄ Mo
fw	1141.80	1111.73	1111.73	1105.77	1098.73	1215.88
space group	<i>Cc</i> (No. 9)	<i>P2₁/n</i> (No. 14)	<i>P2₁/n</i> (No. 14)	<i>P2₁/n</i> (No. 14)	<i>P2₁/n</i> (No. 14)	<i>P</i> $\bar{1}$ (No. 2)
<i>a</i> (Å)	23.936(3)	12.073(7)	11.498(4)	12.258(2)	14.75(1)	11.349(5)
<i>b</i> (Å)	12.244(4)	22.55(2)	27.625(6)	22.932(3)	17.336(9)	14.251(4)
<i>c</i> (Å)	20.348(2)	19.497(9)	17.059(2)	19.710(2)	21.587(10)	18.731(5)
α (deg)	90	90	90	90	90	88.07(2)
β (deg)	109.520(8)	104.94(4)	99.95(2)	104.808(8)	110.20(4)	86.39(3)
γ (deg)	90	90	90	90	90	88.87(3)
<i>V</i> (Å ³)	5620(1)	5129(5)	5336(2)	5356(1)	5181(4)	3021(1)
<i>Z</i>	4	4	4	4	4	2
ρ_{calc} (g cm ⁻³)	1.349	1.440	1.384	1.371	1.408	1.336
<i>F</i> (000)	2360	2288	2288	2288	2272	1260
μ_{calc} (cm ⁻¹)	4.02	4.38	4.21	4.19	4.35	3.81
cryst size (mm ³)	1.0 × 0.8 × 0.6	0.6 × 0.15 × 0.1	0.6 × 0.15 × 0.05	0.4 × 0.3 × 0.2	0.6 × 0.3 × 0.2	0.8 × 0.2 × 0.15
scan type	ω -2 θ	ω -2 θ	ω	ω -2 θ	ω -2 θ	ω -2 θ
2 θ range (deg)	5–55	5–55	5–55	5–50	5–55	5–50
no. measd	6905	12 275	12 839	9895	12 325	11 427
no. unique	6761	11 730	12 242	9426	11 872	10 566
no. obsd	5871	3792	4716	4545	6396	5448
no. var	680	653	666	712	662	743
corrections	Lorentz–polarization; absorption (ψ scan, transmn factor: 0.9219–0.9999); decay (6.3%, linear); secondary extinction (coeff: 4.763 × 10 ⁻⁸)	Lorentz–polarization; absorption (ψ scan, transmn factor: 0.9521–0.9965)	Lorentz–polarization	Lorentz–polarization; absorption (ψ scan, transmn factor: 0.9447–0.9996)	Lorentz–polarization; absorption (ψ scan, transmn factor: 0.9379–0.9988)	Lorentz–polarization; absorption (ψ scan, transmn factor: 0.9621–0.9986)
<i>R</i> ^a	0.030	0.058	0.048	0.047	0.047	0.044
<i>R</i> _w ^b	0.031	0.057	0.045	0.047	0.044	0.037
GOF	1.68	1.57	1.31	1.44	1.60	1.41
residual peaks (e ⁻ /Å ⁻³)	0.39, –0.46	0.85, –0.89	0.40, –0.36	0.31, –0.38	0.89, –0.42	0.35, –0.33

^a $R = \sum ||F_o| - |F_c|| / \sum |F_o|$. ^b $R_w = [\sum w(|F_o| - |F_c|)^2 / \sum w F_o^2]^{1/2}$.

placed at the calculated positions and included in the final stages of the refinements with fixed parameters.

Acknowledgment. This work was supported by the Ministry of Education, Science, Sports, and Culture of Japan (Grant Nos. 09102004 and 09238103).

Supporting Information Available: Tables of atomic coordinates and equivalent thermal parameters, anisotropic thermal parameters, and extensive bond lengths and angles, together with figures with full atom-numbering schemes, for **7**, **10a**, **12a**, **13b**, **14**·THF, and **15**·Et₂O. These materials are available free of charge via the Internet at <http://pubs.acs.org>.

OM000049D